Insights into Magnetically Induced Current Pathways and Optical Properties of Isophlorins

ARTICLE *in* THE JOURNAL OF PHYSICAL CHEMISTRY A · SEPTEMBER 2013

Impact Factor: 2.69 · DOI: 10.1021/jp404828n · Source: PubMed

3 AUTHORS:

Rashid Valiev
Tomsk State University
22 PUBLICATIONS **86** CITATIONS
SEE PROFILE

Heike Fliegl
University of Oslo
36 PUBLICATIONS **851** CITATIONS
SEE PROFILE

Dage Sundholm
University of Helsinki
205 PUBLICATIONS **4,623** CITATIONS
SEE PROFILE

THE JOURNAL OF PHYSICAL CHEMISTRY A

Article

pubs.acs.org/JPCA

Insights into Magnetically Induced Current Pathways and Optical Properties of Isophlorins

Rashid R. Valiev,*[,†,‡] Heike Fliegl,*[,§] and Dage Sundholm*[,∥]

[†]National Research Tomsk Polytechnic University, 43a Lenin Avenue, Building 2, Tomsk 634050, Russian Federation

[‡]Tomsk State University, Lenina Avenue 36, Tomsk 634050, Russian Federation

[§]Centre for Theoretical and Computational Chemistry (CTCC), Department of Chemistry, University of Oslo, P.O. Box 1033 Blindern, 0315 Oslo, Norway

[∥]Department of Chemistry, University of Helsinki, P.O. Box 55 (A. I. Virtanens plats 1), FIN-00014 University of Helsinki, Finland

Supporting Information

ABSTRACT: The magnetically induced current density of tetraoxa-isophlorin and dioxa-dithia-isophlorin have been studied at the density functional theory (DFT) level using the gauge including magnetically induced current method (GIMIC). The current density calculations show that the studied isophlorins with formally 28 π electrons are strongly antiaromatic, sustaining paratropic ring currents of −48.5 and −58.3 nA/T, respectively. All chemical bonds of the porphyrinoid macroring participate in the transport of the paratropic ring current. Calculations of excitation energies at the time-dependent density functional theory (TDDFT) level and at correlated ab initio levels show that tetraoxa-isophlorin and dithia-isophlorin have small optical gaps of 0.82−1.34 and 0.90−1.25 eV, respectively. The transition to the lowest excited state, which belongs to the B_g irreducible representation, is dipole forbidden and has therefore not been observed in the spectroscopical studies. For dioxa-dithia-isophlorin, the excitation energies of the Q and B bands calculated at the TDDFT level agree rather well with experimental values with deviations in the range of [−0.15, +0.27] eV, whereas corresponding excitation energies obtained at the ab initio levels are 0.14−0.51 eV too large as compared to experimental values. For tetraoxa-isophlorin, the deviations of the TDDFT excitation energies from experimental values are in the range [−0.10, +0.50] eV and the ab initio values are 0.53−0.97 eV larger than the experimental values due to the significant double excitation character of the excited states.

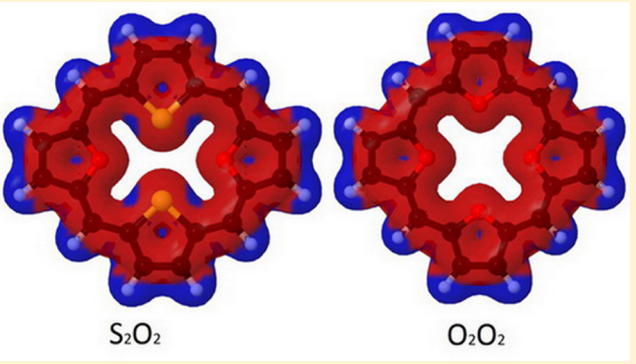

1. INTRODUCTION

Aromatic molecules sustain a net diatropic ring current when exposed to an external magnetic field. The diatropic current direction is defined as the current flow that induces a magnetic field opposed to the applied external one. The magnitude and direction of the ring current can be used for assessing and quantifying the degree of aromaticity according to the magnetic criterion.[1] Molecules that sustain net paratropic ring currents, i.e., ring currents that flow in the nonclassical direction, are considered antiaromatic. Aromatic molecules are common as the diatropic ring current stabilizes the molecule, whereas antiaromatic molecules are rare. Planar and aromatic molecules fulfill the Hückel rule of aromaticity when having $4N + 2$ π electrons in the molecular ring. The classical example of antiaromatic molecules is cyclobutadiene (C_4H_4), which has four π electrons and fulfills the Hückel rule of $4N$ π electrons for antiaromaticity. Cyclobutadiene is actually not a very good example of antiaromatic molecules, because the unsubstituted C_4H_4 has not been synthesized. The recent synthesis of dimethylated cyclobutadiene has been questioned by experimentalists and computational chemists alike.[2−6] Cyclobutadiene is also difficult to study computationally due to the near-degeneracy of low-lying states.[7]

Cyclododecatrienetriyne with its 12 π electrons is a better example of antiaromatic molecules, because it has been synthesized and characterized spectroscopically. The ^{1}H NMR chemical shifts of the HC═CH moieties are 1.2 ppm higher than those for the $H_2C═CH_2$ molecule indicating that the ring current of the macroring is paratropic.[8,9] Multiring antiaromatic molecules consisting of cyclododecatrienetriyne rings fused with benzene rings have also been proposed.[10,11] The cyclododecatrienetriyne−benzene moieties are the basic building units for two-dimensional graphyne layers,[12] which is an interesting form of carbon. An octahedral all-carbon molecule with cyclododecatrienetriyne building units has recently been proposed.[13]

Received: May 16, 2013
Revised: August 16, 2013

dx.doi.org/10.1021/jp404828n | J. Phys. Chem. A XXXX, XXX, XXX−XXX

Isophlorins are porphyrin derivatives that were predicted by Woodward already in 1960.[14] They retain the conjugated network of the free-base porphyrin, but their electronic properties differ from the porphyrin ones because their anticipated aromatic pathway consists of 20 π electrons, which leads to an antiaromatic character of the porphynoid ring according to Hückel's $4N + 2$ π electron rule. Also other types of 20 π electron heteroporphyrins exist.[15] Isophlorins are generally instable with respect to oxidation. The oxidation of isophlorins yields more stable aromatic porphynoids with a traditional aromatic pathway of 18 π electrons. Recently, Reddy and Anand reported the synthesis of air-stable isophlorins.[16] Tetraoxa-isophlorin and dioxa-dithia-isophlorin represent large antiaromatic molecules with all four pyrrole nitrogens of the porphyrins replaced by either oxygen or sulfur.[16−19] The pentafluorophenyl substituents in the meso positions stabilize the isophlorins because they withdraw electrons from the isophlorin macroring. The synthesized isophlorins are planar antiaromatic molecules that might constitute a new promising class of conjugated macrocycles.[20]

For molecules consisting of fused or connected molecular rings, the ring current has the possibility to take different routes. For molecules with several plausible current pathways, reliable information about the current pathway is hard to assess experimentally, whereas numerical integration of calculated current densities yields unambiguous information about the pathways of the current flow. Current−density calculations on porphyrins and twisted hexaphyrins showed that not a single pathway is responsible for the current transport around the macroring.[21−26] The calculations also showed that the aromatic or antiaromatic character of the Möbius twisted hexaphyrins depends on the topology and the total number of π electrons.[22,23]

The aim of this work is to computationally investigate spectroscopic and magnetic properties of the recently synthesized tetraoxa-isophlorin and dioxa-dithia-isophlorin,[16] using density functional theory (DFT). The gauge-including magnetically induced current (GIMIC) method[27,28] has been employed to elucidate the aromatic character and pathways of the isophlorins. An overview of the GIMIC method and applications of the method are given in ref 29. We also report vertical excitation energies that have been calculated and compare them to experimental values deduced from UV−vis spectra.

2. COMPUTATIONAL METHODS

The molecular structures were optimized at the density functional theory (DFT) level using Becke's three-parameter functional (B3LYP)[30] as implemented in Turbomole version 6.4.[31] The Karlsruhe triple-ζ quality basis sets augmented with polarization functions (def2-TZVP)[32] have been employed in the calculations. The prefix def2 is omitted in the following.

Vertical excitation energies were calculated at the linear-response time-dependent DFT (TDDFT) level using the same functional and basis sets. The electronic excitation energies were also calculated at ab initio correlated levels employing the second-order algebraic diagrammatic construction ADC(2) and the linear-response approximate singles and doubles coupled-cluster (CC2) calculations. The resolution of the identity approximation was employed to speed up the calculations.[33−35] The reduced-virtual-space (RVS) approach with an energy threshold of 50 eV[36] was used in the ADC(2) and CC2 calculations, making the ab initio correlation calculations on the large substituted porphyrinoids feasible. All calculations have been performed with Turbomole.[31]

Nuclear magnetic shieldings were calculated using the B3LYP functional and the TZVP basis set. Magnetically induced current densities were calculated using the GIMIC method.[27,28] GIMIC is an independent program that uses the magnetically perturbed density matrices from nuclear magnetic shielding calculations, the one-electron density matrix, and basis-set information as input data.[27,28] The ring-current strength and current pathways were determined by numerical integration of the current−density susceptibility (in nA/T) passing through cut planes perpendicularly to selected bonds of the isophlorins. The current−density susceptibility is called current density in the rest of the paper. Plots of the modulus of the current densities were generated with JMOL.[37] The pictures of the current pathways were obtained with GIMP.[38]

3. MOLECULAR STRUCTURES AND NOMENCLATURE

The molecular structures of the isophlorins were optimized at the B3LYP/TZVP level. The obtained structures agree well with experimental X-ray diffraction data.[16] The Cartesian coordinates are given as Supporting Information. The molecular structures of $S_2O_2-C_6F_5$ and $O_2O_2-C_6F_5$ were assumed to belong to the C_{2h} point group. The abbreviations $S_2O_2-C_6F_5$ and $O_2O_2-C_6F_5$ stand for the dioxa-dithia-isophlorin and tetraoxa-isophlorin substituted with fluorinated phenyl groups in the meta positions. Dioxa-dithia-isophlorin and tetraoxa-isophlorin without the C_6F_5 groups are analogously denoted S_2O_2 and O_2O_2. Frequency calculations for the optimized structures of $S_2O_2-C_6F_5$ and $O_2O_2-C_6F_5$ yielded small imaginary frequencies related to rotations of the C_6F_5 groups. See Supporting Information. Small rotational changes in the orientation of the phenyl groups are not expected to significantly affect the results of the current density calculations nor the calculated excitation energies. The molecular structures of S_2O_2 and O_2O_2 were optimized at the B3LYP/TZVP level in the D_{2h} and C_{2h} point groups, respectively. The obtained structures for S_2O_2 and O_2O_2 are minima on the potential energy surface.

4. CURRENT−DENSITY CALCULATIONS

Plots of the signed modulus of the current densities of S_2O_2 and O_2O_2 are shown in Figure 1. The current density plots for

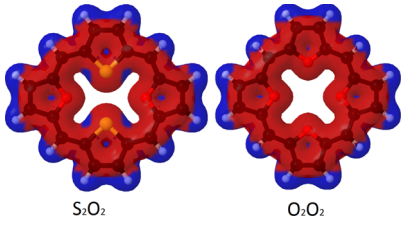

Figure 1. Signed modulus of the magnetically induced current densities for S_2O_2 and O_2O_2. Diatropic currents are shown in blue and paratropic currents in red.

$S_2O_2-C_6F_5$ and $O_2O_2-C_6F_5$ are very similar. As for the previously studied porphyrinoids,[21−23,26] the diatropic current flows along the outer edge of the molecular macroring and the paratropic one in the interior of it. For the investigated isophlorins, the very strong paratropic currents inside the molecular ring dominates suggesting that the isophlorins are

dx.doi.org/10.1021/jp404828n | J. Phys. Chem. A XXXX, XXX, XXX−XXX

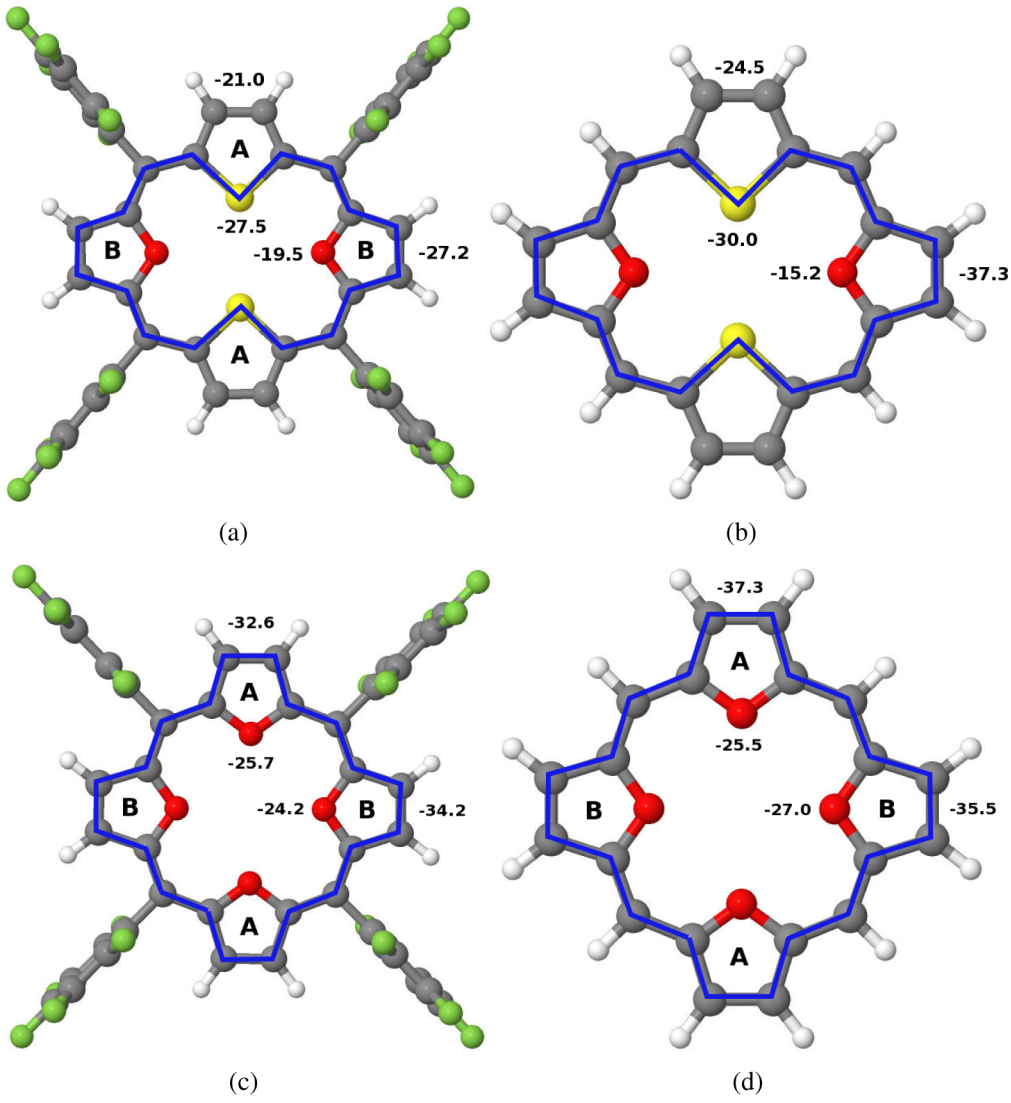

Figure 2. Main current pathways for (a) $S_2O_2-C_6F_5$, (b) S_2O_2, (c) $O_2O_2-C_6F_5$, and (d) O_2O_2 are indicated with the blue line. The integrated current strengths for the inner and outer routes of rings A and B are also given.

antiaromatic, which is in line with the experimental assignment.[16]

The calculated current pathways for $S_2O_2-C_6F_5$ and $O_2O_2-C_6F_5$ are depicted in Figure 2, and the corresponding current strengths (in nA/T) are given in Table 1.

4.1. S_2O_2 and $S_2O_2-C_6F_5$. The strengths of the current density passing selected bonds are given in Table 1. For $S_2O_2-C_6F_5$, the ring-current strength at the thiophene ring (ring A) is −48.5 nA/T, which agrees well with the current strength of −46.7 nA/T passing the furan ring (ring B). The deviation between the two values is less than 4%, showing that the charge conservation condition is almost fulfilled at the B3LYP/TZVP level for such a large molecule. The charge conservation condition is satisfied only in the limit of complete basis sets. The strong negative currents indicate that the molecule is antiaromatic according to the ring-current criterion.

Integration of the current density shows that the current pathways for S_2O_2 and $S_2O_2-C_6F_5$ fork into an outer and an inner route at the A and B subrings, which is a similar behavior as we previously obtained for porphyrins and hexaphyrins.[21−23] For the thiophene ring (A), the current flow of −27.5 nA/T via the inner route is 6.5 nA/T stronger than the current passing the C−C bond, whereas for the furan ring (B) the current strength of −27.2 nA/T along the outer route is 7.7 nA/T stronger than the one passing the oxygen, suggesting that the resistance of the oxygen moiety of the furan ring is significantly larger than that for the sulfur of the thiophene ring. For $S_2O_2-C_6F_5$, the difference of 6−7 nA/T in current strengths of the inner and outer routes is somewhat smaller than the ones of 10−11 nA/T we obtained for the porphyrins.[21] For the unsubstituted S_2O_2, more than two-thirds of the current takes the outer route at the furan ring.

S_2O_2 sustains a ring current that is 6 nA/T stronger than the meso substituted one. The integration of the current density shows that the stronger current mainly originates from an increase in the paratropic ring-current contribution, whereas the strength of the diatropic current is almost unaffected by the meso substituents. The weaker ring current of the isophlorins with C_6F_5 substituents is due to the electron attracting fluorines of the substituents, which remove electrons from the isophlorin macroring rendering it less antiaromatic. This is in line with previous findings regarding fluorination effects upon current densities of fluorinated hydrocarbon multirings.[39]

dx.doi.org/10.1021/jp404828n | J. Phys. Chem. A XXXX, XXX, XXX−XXX

Table 1. Calculated Current Strengths (I_1 and I_2, nA/T) for Selected Bonds of S_2O_2, O_2O_2, $S_2O_2-C_6F_5$, and $O_2O_2-C_6F_5$, Where I_1 and I_2 Are the Current Strengths of the Inner and the Outer Routes, Respectively

S_2O_2		$S_2O_2-C_6F_5$	
thiophene (A)		tiophene (A)	
total	−54.5	total	−48.5
I_1	−24.5	I_1	−21.0
I_2	−30.0	I_2	−27.5
furan (B)		furan (B)	
total	−52.5	total	−46.7
I_1	−37.3	I_1	−27.2
I_2	−15.2	I_2	−19.5
O_2O_2		$O_2O_2-C_6F_5$	
furan (A)		furan (A)	
total	−62.8	total	−58.3
I_1	−37.3	I_1	−32.6
I_2	−25.5	I_2	−25.7
furan (B)		furan (B)	
total	−62.5	total	−58.2
I_1	−35.5	I_1	−34.2
I_2	−27.0	I_2	−24.2

The strength of the diatropic contribution to the ring current of free-base porphyrin about 40.9 nA/T, which is only 17.2 nA/T larger than the diatropic contribution to the ring current of $S_2O_2-C_6F_5$. However, the paratropic contribution of −72.3 nA/T is the dominating contribution to the ring current of the isophlorin in comparison with the paratropic contribution of −13.7 nA/T for free-base porphyrin.

4.2. O_2O_2 and $O_2O_2-C_6F_5$. As the molecular structure of $O_2O_2-C_6F_5$ belongs to the C_{2h} point group, the inner oxygens of the furan rings are not completely equivalent. However, the difference in the current strengths passing the oxygens of ring A and B is only 1.5 nA/T. The total current strength of $O_2O_2-C_6F_5$ is −58.3 nA/T, which is about 10 nA/T stronger than that for $S_2O_2-C_6F_5$. Thus, $O_2O_2-C_6F_5$ can be considered to be somewhat more antiaromatic than $S_2O_2-C_6F_5$ according to the ring-current criterion. The sulfur containing isophlorins sustain weaker ring currents because sulfur is a softer donor than oxygen.

Calculations of the current pathways of O_2O_2 and $O_2O_2-C_6F_5$ show that the ring currents fork into inner and outer routes at rings A and B. For the tetraoxa-isophlorins, the outer route at the four furan rings is the main current pathway. At furan ring A, the pathway splits into outer and inner currents of −32.6 and −25.7 nA/T, respectively. At furan ring B, very similar current strengths of −34.2 and −24.2 nA/T are obtained. Thus, the calculated ring-current strengths of −62.8 and −58.3 nA/T for the O_2O_2 molecules are about 10 nA/T stronger than those for the corresponding S_2O_2 species. For the tetraoxa-isophlorins, the C_6F_5 substituents have a smaller effect on the ring-current strength. The ring-current strength of $O_2O_2-C_6F_5$ is only 4−5 nA/T weaker than that for the unsubstituted tetraoxa-isophlorin. The substitution does not alter the main current pathway either. The pentafluorophenyl groups do not have a strong influence on the current pathway. The current strengths of the tetraoxa-isophlorins are also less affected by the pentafluorophenyl substituents than for dioxa-dithia-isophlorin.

5. ^{1}H NMR CHEMICAL SHIFTS

Calculations of the nuclear magnetic shieldings for $S_2O_2-C_6F_5$ and $O_2O_2-C_6F_5$ yield ^{1}H NMR chemical shifts of −0.04, +0.30 ppm and −1.87, −1.29 ppm, respectively. The nuclear magnetic shielding for the hydrogens of the tetramethylsilan (TMS) reference calculated at the same level of theory is 31.91 ppm. The experimental ^{1}H NMR chemical shifts for $S_2O_2-C_6F_5$ and $O_2O_2-C_6F_5$ are 3.33, 3.37, and 2.49 ppm, respectively.[16] Comparison of calculated and experimental data indicates that the paratropic current sustained by isophlorins under the experimental conditions is somewhat weaker than that obtained in the DFT calculation for a single molecule. The ring-current strength of the isophlorins under experimental conditions can be estimated by assuming that the ^{1}H NMR chemical shifts at the β carbons of the porphyrinoids depend linearly on the ring-current strength.[?] The average ^{1}H NMR chemical shielding for the outer hydrogens of free-base porphyrin calculated at the B3LYP/TZVP level is 20.91 ppm[21] and the corresponding average ring-current strength is 27.35 nA/T. For $O_2O_2-C_6F_5$, the average of the calculated ^{1}H NMR chemical shieldings is 33.50 ppm. For $S_2O_2-C_6F_5$, the average of the calculated ^{1}H NMR chemical shieldings is 31.79 ppm. Using the ring-current strength of −58.3 nA/T for $O_2O_2-C_6F_5$ and the average ring-current strength of free-base porphyrin as well as the chemical shielding of 31.79 ppm for the hydrogens at the β carbons of $S_2O_2-C_6F_5$, a ring-current strength of −46.6 nA/T is estimated for $S_2O_2-C_6F_5$ by linear interpolation. The interpolated current strength of −46.6 nA/T agrees rather well with the calculated value of −48.5 nA/T. The same procedure can be used to estimate the ring-current strength for $S_2O_2-C_6F_5$ and $O_2O_2-C_6F_5$ under the experimental conditions. Linear interpolation using the experimental ^{1}H NMR chemical shifts for $S_2O_2-C_6F_5$ and $O_2O_2-C_6F_5$ and the calculated ^{1}H NMR chemical shielding for TMS yields estimated ring-current strengths of −24.8 nA/T and −30.5 nA/T for $S_2O_2-C_6F_5$ and $O_2O_2-C_6F_5$, respectively. Thus, $S_2O_2-C_6F_5$ and $O_2O_2-C_6F_5$ are strongly antiaromatic also under the experimental conditions.

The main reasons for the discrepancy are solvent shifts, C−H···F hydrogen bonding, and vibrational corrections. The surrounding solvent molecules most likely decrease the paratropic ring current as the electron-rich isophlorins are stabilized by donating electrons toward its surroundings. Nevertheless, the current densities calculated for the molecules in the gas phase can be expected to yield the correct current pathway pattern.

6. EXCITATION ENERGIES

6.1. Experimental Data. The experimental excitation energies and oscillator strengths have been deduced from the measured absorption spectra of $S_2O_2-C_6F_5$ and $O_2O_2-C_6F_5$ reported in ref 16. The experimental oscillator strengths were estimated using[40]

$$f = 4.32\cdot10^{-9}\int \varepsilon \, d\nu \qquad (1)$$

where f is the oscillator strength. The integral is approximated as $\int \varepsilon \, d\nu = \varepsilon_{max}\Delta\nu_{1/2}$. ε_{max} (M^{-1} cm^{-1}) is the extinction coefficient at the peak maximum and $\Delta\nu_{1/2}$ (cm^{-1}) is the half-width of the spectral line. The uncertainty of the experimental oscillator strengths obtained using eq 1 is less than 6%.[40] The vertical excitation energies are assumed to be at the peak maxima. The calculated excitation energies and oscillator

dx.doi.org/10.1021/jp404828n | J. Phys. Chem. A XXXX, XXX, XXX−XXX

Table 2. Vertical Excitation Energies (eV) for $S_2O_2-C_6F_5$ and $O_2O_2-C_6F_5$ in the Gas Phase Calculated at the B3LYP, ADC(2), and CC2 Levels Using the TZVP Basis Set (Oscillator Strengths f in Parentheses)

state	band	B3LYP	ADC(2)	CC2	experiment[16]
			$S_2O_2-C_6F_5$		
1 (B_g)		0.90 (0.00)	1.24 (0.00)	1.25 (0.00)	
2 (A_u)	Q_x	2.52 (0.08)	2.86 (0.25)	3.08 (0.14)	2.67 (0.02−0.04)
3 (B_u)	Q_y	2.96 (0.08)	3.27 (0.17)	3.37 (0.07)	2.85 (0.02−0.04)
4 (B_u)	B_x	3.50 (0.40)	3.98 (0.60)	3.80 (0.90)	3.47 (0.30−0.60)
5 (B_u)	B_y	3.60 (0.50)	4.01 (1.27)	4.15 (1.26)	3.87 (0.33−0.60)
			$O_2O_2-C_6F_5$		
1 (B_g)		0.82 (0.00)	1.34 (0.00)	1.26 (0.00)	
2 (A_u)	Q_x	2.57 (0.06)	3.21 (0.46)	3.20 (0.26)	2.67 (0.02−0.04)
3 (B_u)	Q_y	3.09 (0.08)	3.72 (0.30)	3.66 (0.20)	2.83 (0.02−0.04)
4 (B_u)	B_x	3.80 (1.30)	3.90 (1.31)	4.03 (1.36)	3.30 (0.30−0.4)
5 (B_u)	B_y	4.09 (1.24)	4.50 (1.38)	4.57 (1.34)	3.60 (0.33−0.4)

strengths of $S_2O_2-C_6F_5$ and $O_2O_2-C_6F_5$ are compared to experimental values in Table 2.

Table 2 shows that the most significant discrepancy between calculated and measured excitation energies is the missing $1^1A_g \rightarrow 1^1B_g$ transition in the recorded spectrum, because the $^1A_g \rightarrow {}^1B_g$ transition is dipole forbidden rendering the experimental detection difficult. For free-base porphyrin, the first $^1B_{1g}$ state is much higher in energy with an excitation energy of 2.90 eV, according to DFT calculations.[41]

6.2. $S_2O_2-C_6F_5$. The excitation energies of $S_2O_2-C_6F_5$ calculated at the ADC(2) and CC2 levels are 0.21−0.68 eV larger than the vertical excitation energies deduced from the experimental UV−vis spectrum, whereas the B3LYP excitation energies agree within 0.13−0.20 eV with experiment. The oscillator strengths calculated at the B3LYP level are also in qualitative agreement with the ones obtained experimentally, whereas at the ADC(2) and CC2 levels the oscillator strengths for the Q_x and Q_y bands are up to an order of magnitude larger than the ones deduced from the experimental spectrum. For the B_x and B_y bands, the ab initio calculations yield oscillator strengths that are about a factor of 2−3 too large as compared to experiment.

The calculated excitation energies and oscillator strengths show that the transitions of the Q and B bands of $S_2O_2-C_6F_5$ can be simulated using the TDDFT B3LYP calculations, whereas the ab initio response calculations more or less fail to describe the transitions of the B bands due to the significant double excitation character of the transition from the ground to the excited states. See the Supporting Information.

6.3. $O_2O_2-C_6F_5$. For $O_2O_2-C_6F_5$, the excitation energies obtained at the ab initio levels are 0.50−0.98 eV larger than the experimental values. The oscillator strengths for the Q_x and Q_y bands calculated at the ADC(2) and CC2 levels are an order of magnitude too large as compared to experiment, whereas for the B_x and B_y bands they are 3−4 times larger than those obtained in the experiment. The excitation energies for the Q_x and Q_y bands calculated at the B3LYP level agree rather well with the experimental values with discrepancies of only 0.13−0.29 eV, whereas for the B_x and B_y bands the deviation between the experimental vertical excitation energies and the B3LYP ones is 0.5 eV. At the B3LYP level, the oscillator strengths for the Q_x and Q_y bands are also in fair agreement with the experimental ones, whereas for the B_x and B_y bands they are also 3−4 times larger than the ones deduced from the experimental spectrum.

The calculated excitation energies and oscillator strengths show that the B3LYP excitation energies and band strengths of the Q bands largely agree with experimental data, whereas the B bands of $O_2O_2-C_6F_5$ are not accurately calculated at the B3LYP, ADC(2), or CC2 levels. There is a bathochromic shift (0.14−0.80 eV) of the Soret band for the S_2O_2 and O_2O_2 molecules as compared with the 18 π porphyrins.,[42] which agrees with the conclusions drawn by Kakui and co-workers,[43] who showed that the Soret band of 16 π porphyrinoids is substantially blue-shifted as compared with 18 π porphyrins. Also, the Q bands are not well described at the ab initio levels. For free-base porphyrins, the contributions from double excitations are smaller yielding a much better agreement between CC2 excitation energies and experimental values.[42]

The large oscillator strengths obtained for the Q bands indicate an incorrect mixing of the low-lying excited states due to an insufficient description of high-order correlation effects. Thus, computational levels considering high-order correlation effects have to be employed when aiming at a good agreement between calculated and measured excitation spectra for the isophlorins in the energy range of the Q and B bands.

7. SUMMARY AND CONCLUSIONS

Magnetically induced current densities of dioxa-dithia-isophlorin ($S_2O_2-C_6F_5$) and tetraoxa-isophlorin ($O_2O_2-C_6F_5$) have been studied by employing gauge including magnetically induced current (GIMIC) calculations. The analysis of the current density confirms that both molecules are antiaromatic. GIMIC calculations of the ring-current strengths show that $O_2O_2-C_6F_5$ is somewhat more antiaromatic than $S_2O_2-C_6F_5$. The ring-current pathways around the macromolecular ring were obtained by numerical integration of the current flow passing chemical bonds of the molecular ring. The strength of the paratropic ring currents of $S_2O_2-C_6F_5$ and $O_2O_2-C_6F_5$ are −48.5 and −58.3 nA/T, which are 4 and 5 times stronger than those for benzene, respectively.

Calculations of the current strengths show that all chemical bonds of the porphyrinoid macroring participate in the transport of the paratropic current. The current flow splits at the oxygen and sulfur containing five-membered rings into an outer and inner pathway. The preferred current route for the furan type subrings is on the outside of the ring along the C−C bond, but the opposite is the case for the thiophene type rings. However, all chemical bonds of the macroring participate in the current transport as 29−45% of current takes the inner route of

dx.doi.org/10.1021/jp404828n | J. Phys. Chem. A XXXX, XXX, XXX−XXX

the furan rings and about 45% of the current flows via the outer route of the thiophene rings.

Comparison of the current strengths for $S_2O_2-C_6F_5$, $O_2O_2-C_6F_5$, and the unsubstituted ones shows the effect of the pentafluorophenyl substitution on current pathways and current strengths. For $O_2O_2-C_6F_5$ the pentafluorophenyl groups reduce the current strength by 6%, whereas for $S_2O_2-C_6F_5$ the ring current is 11% weaker than that for S_2O_2.

Calculations of the vertical excitation energies and oscillator strengths using density functional theory and ab initio methods yielded a dipole forbidden $A_g \rightarrow B_g$ transition as the lowest excited state. At the B3LYP level, the antiaromatic isophlorin has a small optical gap of 0.90 eV, whereas the experimental energies of the dipole allowed transitions of the Q and B bands are in the range 2.67−3.87 eV. The excitation energies calculated at the ADC(2) and CC2 levels are systematically much larger due to the significant contributions from double excitations, especially for $O_2O_2-C_6F_5$. The excitation energies and oscillator strengths of the Q and B bands for $S_2O_2-C_6F_5$ calculated at the B3LYP level are in fair agreement with experimental values. For $O_2O_2-C_6F_5$, the B3LYP excitation energies and oscillator strengths of the Q-band agree well with experiment, whereas for the B band the calculated excitation energies and oscillator strengths are much larger than the experimental ones at all the employed computational levels.

■ ASSOCIATED CONTENT

Ⓢ Supporting Information

Structures, Cartesian coordinates, harmonic frequencies, nuclear magnetic shieldings, and single and double excitation conributions to the excited states of the studied molecules. This information is available free of charge via the Internet at http://pubs.acs.org/.

■ AUTHOR INFORMATION

Corresponding Authors

*R. R. Valiev: e-mail, valievrashid@mail.ru.
*H. Fliegl: e-mail, Heike.Fliegl@kjemi.uio.no.
*D. Sundholm: e-mail, Dage.Sundholm@helsinki.fi.

Notes

The authors declare no competing financial interest.

■ ACKNOWLEDGMENTS

This research has been supported by the Academy of Finland through its Computational Science Research Programme (LASTU). We thank Magnus Ehrnrooth foundation for financial support. CSC (the Finnish IT Center for Science) is acknowledged for computer time. H.F. is thankful for the support by the Norwegian Research Council through the CoE Centre for Theoretical and Computational Chemistry (Grant No. 179568/V30). This work has received support from the Norwegian Supercomputing Program (NOTUR) through a grant of computer time (Grant No. NN4654K).

■ REFERENCES

(1) Fliegl, H.; Sundholm, D.; Taubert, S.; Jusélius, J.; Klopper, W. Magnetically Induced Current Densities in Aromatic, Antiaromatic, Homoaromatic, and Nonaromatic Hydrocarbons. *J. Phys. Chem. A* **2009**, *113*, 8668−8676.

(2) Legrand, Y.-M.; van der Lee, A.; Barboiu, M. Single-Crystal X-ray Structure of 1,3-Dimethylcyclobutadiene by Confinement in a Crystalline Matrix. *Science* **2010**, *329*, 299−302.

(3) Legrand, Y.-M.; Dumitrescu, D.; Gilles, A.; Petit, E.; van der Lee, A.; Barboiu, M. Reply to A Computational Evaluation of the Evidence for the Synthesis of 1,3-Dimethylcyclobutadiene in Solid State and Aqueous Solution -Beyond the Experimental Reality. *Chem.—Eur. J.* **2013**, *19*, 4938−4941.

(4) Legrand, Y.-M.; Dumitrescu, D.; Gilles, A.; Petit, E.; van der Lee, A.; Barboiu, M. A Constrained Disorder Refinement: - Reinvestigation of "Single-Crystal X-ray Structure of 1,3-Dimethylcyclobutadiene" by M. Shatruk and I. V. Alabugin. *Chem.—Eur. J.* **2013**, *19*, 4946−4950.

(5) Shatruk, M.; Alabugin, I. V. Reinvestigation of "Single-Crystal X-ray Structure of 1,3-dimethylcyclobutadiene. *Chem.—Eur. J.* **2013**, *19*, 4942−4945.

(6) Rzepa, H. S. A Computational Evaluation of the Evidence for the Synthesis of 1,3-Dimethylcyclobutadiene in the Solid State and Aqueous Solution. *Chem.—Eur. J.* **2013**, *19*, 4932−4937.

(7) Pathak, S.; Bast, R.; Ruud, K. Multiconfigurational Self-Consistent Field Calculations of the Magnetically Induced Current Density Using Gauge-Including Atomic Orbitals. *J. Chem. Theory Comput.* **2013**, *9*, 2189−2198.

(8) Untch, K. G.; Wysocki, D. C. Cyclododecatrienetriyne. *J. Am. Chem. Soc.* **1966**, *88*, 2608−2610.

(9) Pople, J. A.; Untch, K. G. *J. Am. Chem. Soc.* **1966**, *88*, 4811−4815.

(10) Baughman, R. H.; Eckhardt, H.; Kertesz, M. Structure-property predictions for new planar forms of carbon: Layered phases containing sp^2 and sp atoms. *J. Chem. Phys.* **1987**, *87*, 6687−6699.

(11) Jusélius, J.; Sundholm, D. Polycyclic Antiaromatic Hydrocarbon. *Phys. Chem. Chem. Phys.* **2008**, *10*, 6630−6634.

(12) Li, G.; Li, Y.; Liu, H.; Guo, Y.; Li, Y.; Zhu, D. Architecture of graphdiyne nanoscale films. *Chem. Commun.* **2010**, *46*, 3256−3258.

(13) Sundholm, D. C_{72}: Gaudiene a Hollow and Aromatic All-Carbon Molecule. *Phys. Chem. Chem. Phys.* **2013**, *15*, 9025−9028.

(14) Woodward, R. B. Totalsynthese des chlorophylls. *Angew. Chem.* **1960**, *72*, 651−662.

(15) Chang, Y.; Chen, H.; Zhou, Z.; Zhang, Y.; Schütt, C.; Herges, R.; Shen, Z. A 20 π-Electron Heteroporphyrin Containing a Thienopyrrole Unit. *Angew. Chem., Int. Ed.* **2012**, *51*, 12801−12805.

(16) Reddy, J. S.; Anand, V. G. Planar Meso Pentafluorophenyl Core Modified Isophlorins. *J. Am. Chem. Soc.* **2008**, *130*, 3718−3719.

(17) Higashino, T.; Osuka, A. 2,3,17,18-Tetraethylsulfanyl [30]-hexaphyrin(1.1.1.1.1.1) as the first aromatic isophlorin-type free-base. *Chem. Sci.* **2013**, *4*, 1087−1091.

(18) Liu, C.; Shen, D.-M.; Chen, Q.-Y. Synthesis and Reactions of 20 π-Electron β-Tetrakis(trifluoromethyl)-meso-tetraphenylporphyrins. *J. Am. Chem. Soc.* **2007**, *129*, 5814−5815.

(19) Matano, Y.; Nakabuchia, T.; Fujishige, S.; Nakano, H.; Imahori, H. Redox-Coupled Complexation of 23-Phospha-21-thiaporphyrin with Group 10 Metals: A Convenient Access to Stable Core-Modified Isophlorin-Metal Complexes. *J. Am. Chem. Soc.* **2008**, *130*, 16446−16447.

(20) Reddy, J. S.; Anand, V. G. Aromatic Expanded Isophlorins: Stable 30π Annulene Analogues with Diverse Structural Features. *J. Am. Chem. Soc.* **2008**, *131*, 15433−15439.

(21) Fliegl, H.; Sundholm, D. Aromatic Pathways of Porphins, Chlorins and Bacteriochlorins. *J. Org. Chem.* **2012**, *77*, 3408−3414.

(22) Fliegl, H.; Sundholm, D.; Taubert, S.; Pichierri, F. Aromatic Pathways in Twisted Hexaphyrins. *J. Phys. Chem. A* **2010**, *114*, 7153−7161.

(23) Fliegl, H.; Sundholm, D.; Pichierri, F. Aromatic Pathways in Mono- and Bisphosphorous Singly Möbius Twisted [28] and [30]Hexaphyrins. *Phys. Chem. Chem. Phys.* **2011**, *13*, 20659−20665.

(24) Jusélius, J.; Sundholm, D. The aromatic pathways of porphins, chlorins and bacteriochlorins. *Phys. Chem. Chem. Phys.* **2000**, *2*, 2145−2151.

(25) Jusélius, J.; Sundholm, D. The Aromatic Character of Magnesium Porphyrins. *J. Org. Chem.* **2000**, *65*, 5233−5237.

(26) Flieg, H.; Özcan, N.; Mera-Adasme, R.; Pichierri, F.; Jusélius, J.; Sundholm, D. Aromatic pathways in thieno-bridged porphyrins: understanding the influence of the direction of the thiophene ring

on the aromatic character. *Mol. Phys.* **2013**, DOI: 10.1080/00268976.2013.794397.
(27) Jusélius, J.; Sundholm, D.; Gauss, J. Calculation of Current Densities using Gauge-Including Atomic Orbitals. *J. Chem. Phys.* **2004**, *121*, 3952−3963.
(28) Taubert, S.; Sundholm, D.; Jusélius, J. Calculation of spin-current densities using gauge-including atomic orbitals. *J. Chem. Phys.* **2011**, *134*, 054123:1−12.
(29) Fliegl, H.; Taubert, S.; Lehtonen, O.; Sundholm, D. The gauge including magnetically induced current method. *Phys. Chem. Chem. Phys.* **2011**, *13*, 20500−20518.
(30) Lee, C.; Yang, W.; Parr, R. G. Development of the Colle-Salvetti correlation-energy formula into a functional of the electron density. *Phys. Rev. B* **1988**, *37*, 785−789.
(31) Ahlrichs, R.; Bär, M.; Häser, M.; Horn, H.; Kölmel, C. Electronic Structure Calculations on Workstation Computers: The Program System TURBOMOLE. *Chem. Phys. Lett.* **1989**, *162*, 165−169. Current version, see http://www.turbomole.com.
(32) Weigend, F.; Ahlrichs, R. Balanced basis sets of split valence, triple zeta valence and quadruple zeta valence quality for H to Rn: Design and assessment of accuracy. *Phys. Chem. Chem. Phys.* **2005**, *7*, 3297−3305.
(33) Weigend, F.; Häser, M.; Patzelt, H.; Ahlrichs, R. RI-MP2: optimized auxiliary basis sets and demonstration of efficiency. *Chem. Phys. Lett.* **1998**, *294*, 143−152.
(34) Hättig, C.; Weigend, F. CC2 excitation energy calculations on large molecules using the resolution of the identity approximation. *J. Chem. Phys.* **2000**, *113*, 5154−5161.
(35) Hättig, C. Structure optimizations for excited states with correlated second-order methods: CC2 and ADC(2). *Adv. Quantum Chem.* **2005**, *50*, 37−60.
(36) Send, R.; Kaila, V. R. I.; Sundholm, D. Reduction of the virtual space for coupled-cluster excitation energies of large molecules and embedded systems. *J. Chem. Phys.* **2011**, *134*, 214114.
(37) JMOL: an open-source Java viewer for chemical structures in 3D, http://www.jmol.org.
(38) GIMP: GNU Image Manipulation Program, http://www.gimp.org.
(39) Kaipio, M.; Patzschke, M.; Fliegl, H.; Pichierri, F.; Sundholm, D. The effect of fluorine substitution on the aromaticity of polycyclic hydrocarbons. *J. Phys. Chem. A* **2012**, *116*, 10257−10268.
(40) McGlynn, S. P.; Azumi, T.; Kinoshita, M. *Molecular spectroscopy of the triplet state*; Prentice Hall: Englewood Cliffs, NJ, 1969.
(41) Sundholm, D. Interpretation of the electronic absorption spectrum of free-base porphin using time-dependent density-functional theorya. *Phys. Chem. Chem. Phys.* **2000**, *2*, 2275−2281.
(42) Valiev, R. R.; Cherepanov, V. N.; Artyukhov, V. Y.; Sundholm, D. Computational studies of photophysical properties of porphin, tetraphenylporphyrin and tetrabenzoporphyrin. *Phys. Chem. Chem. Phys.* **2012**, *14*, 11508−11517.
(43) Kakui, T.; Sugawara, S.; Hirata, Y.; Kojima, S.; Yamamoto, Y. Anti-Aromatic 16π PorphyrinŰMetal Complexes with meso-Alkyl Substituents. *Chem.—Eur. J.* **2011**, *17*, 7768−7771.